APPLIED PHYSICS LETTERS **87**, 241916 (2005)

Direct evidence of 8:9 commensurate heterojunction formed between InN and AlN on *c* plane

C.-L. Wu, C.-H. Shen, H.-W. Lin, H.-M. Lee, and S. Gwo[a)]
Department of Physics, National Tsing-Hua University, Hsinchu 300, Taiwan, Republic of China

(Received 25 July 2005; accepted 19 October 2005; published online 7 December 2005)

We show that, despite a large difference in lattice constants, high-quality InN/AlN heterostructures can be formed on Si(111) due to the existence of "magic" ratios between the lattice constants of comprising material pairs: 2:1 (Si/Si_3N_4), 5:4 (AlN/Si), and 8:9 (InN/AlN). For InN growth on AlN with nitrogen polarity, by using reflection high-energy electron diffraction and cross-sectional transmission electron microscopy, we have found that the pseudomorphic to commensurate lattice transition occurs within the first monolayer of growth, resulting in an abrupt heterojunction at the atomic scale. This new route of lattice match allows the formation of commensurate and nearly strain-free interface with a common two-dimensional superlattice. © *2005 American Institute of Physics*. [DOI: 10.1063/1.2146062]

Indium nitride (InN) has recently emerged as a promising semiconductor for near-infrared (NIR) optoelectronics because of the newly discovered narrow band gap.[1–7] Also, the superior electron transport properties (low effective mass, high mobility and saturation drift speed) of InN make it very useful for high-frequency, high-speed electronics.[6,8–10] To realize such applications, the ability to grow InN-based heterostructures with high crystalline quality and atomically abrupt interfaces is most critical. However, the large differences in lattice constants (~12% for InN/AlN and ~10% for InN/GaN), the lack of suitable substrates, and the low dissociation/growth temperature of InN post daunting challenges for growing high-quality InN-based heterostructures.

Conventional heteroepitaxy prefers growth of dissimilar materials with closely matched lattice constants and crystal structures, which allows atom-by-atom match across the heterojunction. For example, high-quality heteroepitaxy is possible for a lattice matched system such as $Al_xGa_{1-x}As/GaAs$. On the other hand, for a lattice mismatched system such as $In_xGa_{1-x}As/GaAs$, depending on the amount of mismatch (which is a function of the alloy composition), pseudomorphic growth can be achieved when the overlayer thickness is below a critical thickness beyond which the strain energy will drive the system toward three-dimensional (3D) island growth. Therefore, it is very surprising to find that an AlN buffer layer can significantly improve the structural and electrical properties of grown InN.[5,11,12] In this letter, we demonstrate the possibility of growing high-quality InN/AlN heterostructures with atomically abrupt interfaces on Si(111). We further prove that, within the first monolayer growth of InN on AlN, a perfect 8:9 commensurate interface is formed. In the case of commensurate lattice match (CLM) between two lattices, the ratio of the in-plane lattice constants of the two constituents (a_B/a_A) is close to a rational number m/n.[13] Thus, a common two-dimensional (2D) superlattice (a coincident-site lattice) can be formed at the interface. Recently, the CLM concept has been extensively exploited by us for the systems of Si_3N_4/Si and $AlN/Si_3N_4/Si$ with the "magic" matching ratios of 2:1 (Si/Si_3N_4) and 5:4 (AlN/Si).[14–16]

InN-on-Si samples were grown by plasma-assisted molecular-beam epitaxy (PA-MBE). Three-inch Si(111) wafers were used as the substrates and the base pressure of MBE system was in the 10^{-11} Torr range. Prior to the InN growth, an epitaxial $AlN/\beta\text{-}Si_3N_4$ double-layer structure was grown first on Si. The use of a thin $\beta\text{-}Si_3N_4$ interlayer (~2 nm) is to prevent the formation of an amorphous SiN_x layer and to provide a diffusion barrier against intermixing of group-III elements and Si.[16] A two-stage growth technique of InN was employed: the growth temperature for the initial low-temperature (LT) InN was about 320 °C and that for the subsequent high-temperature (HT) InN was about 520 °C. This technique can effectively suppress the 3D growth mode of InN at the initial stage and ensures the 2D growth mode throughout the growth process. For this work, the III-nitride film thicknesses were 350–650 nm for the InN epilayers and 35–130 nm for the AlN epilayers. The lattice constants of the epilayers determined by x-ray diffraction (XRD) and cross-section transmission electron microscopy (XTEM) are consistent with the formation of relaxed wurtzite InN and AlN epilayers, and the *c* axis is oriented vertically to the Si(111) substrate plane. The in-plane axes of the wurtzite epilayers were found to follow the epitaxial relations: $\langle 11\bar{2}0\rangle_{InN/AlN/Si3N4} \| [\bar{1}10]_{Si}$ and $\langle \bar{1}100\rangle_{InN/AlN/Si3N4} \| [11\bar{2}]_{Si}$.

A key characteristic of the *c* plane of wurtzite lattice is its polarity (the [0001] direction is defined by a vector pointing from group-III atom to nearest-neighbor N atom). Therefore, the (0001) (group-III polarity) and $(000\bar{1})$ (nitrogen polarity, N polarity) surfaces are inequivalent. For the InN epitaxial growth, the surface polarity plays a key role in growth kinetics and film quality. Contrary to the growth of GaN on the *c* plane, Xu and Yoshikawa reported that the growth morphology and film properties of InN grown on a N-polarity surface is more superior than that on an In-polarity surface due to the better thermal stability of N-polarity InN surface, which allows higher growth temperatures (>500 °C).[4,17] To identify the surface polarity, we adopted the technique reported by Smith *et al.* using surface reconstructions and/or polarity-selective wet etching of III-nitrides.[18] Figure 1(a) shows streaky reflection high-energy electron diffraction (RHEED) patterns taken at two

[a)]Electronic mail: gwo@phys.nthu.edu.tw

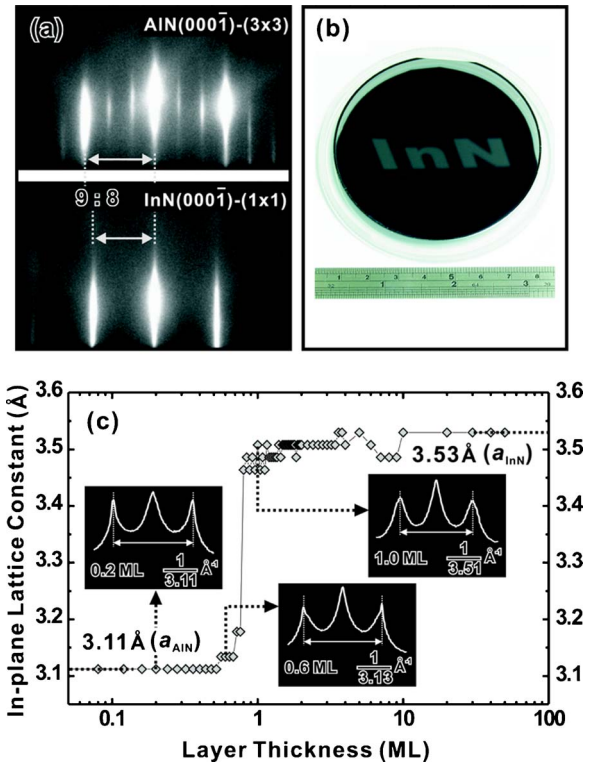

FIG. 1. (a) Static RHEED patterns in the growth process of InN on Si(111) with an AlN/Si_3N_4 double-buffer structure. From top to bottom: AlN(000$\bar{1}$)-(3×3) reconstructed surface at 320 °C (before LT-InN growth) and InN(000$\bar{1}$)-(1×1) surface at 520 °C (after HT-InN growth). The electron beam azimuth is along the $[\bar{1}10]_{Si}$ direction ($\|\langle\bar{1}\bar{1}20\rangle_{InN/AlN}$). (b) Photograph of an InN epitaxial film on 3-in. Si(111), showing a blackish, highly reflective InN surface. The word "InN" shown on the film is a mirror image of "*И*nI" printed on a paper placed nearby. (c) Dynamical RHEED analysis during the first monolayer growth of InN on AlN. Insets within the plot show three corresponding RHEED pattern line profiles.

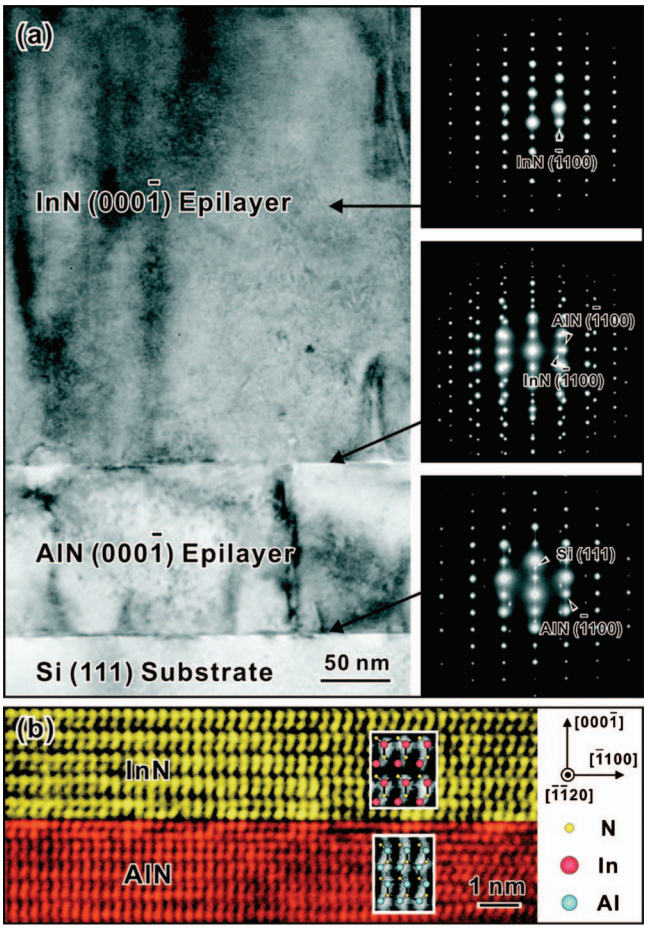

FIG. 2. (Color) (a) XTEM image and SAED patterns of an $InN/AlN/Si_3N_4/Si$ heteroepitaxial structure. (b) High-resolution XTEM image (color-coded) at the InN/AlN interface, indicating that the interface is atomically abrupt and the lattice stacking corresponds to the wurtzite type. Insets are schematic diagrams of wurtzite lattices in comparison to the high-resolution XTEM images of InN and AlN lattice regions.

different growth fronts (AlN versus InN) and Fig. 1(b) displays a photography of a PA-MBE-grown InN film on Si(111). From Fig. 1(a), the ratio of reciprocal lattice constants can be found to be 9:8 (AlN:InN). It should be emphasized that throughout the heteroepitaxial process in our experiments, the RHEED patterns displayed the streaky feature, indicating smooth surface morphologies and 2D growth modes at all growth stages. Moreover, the changes in lattice constant happened very abruptly during the initial heterojunction growth. For the cases of AlN growth on Si_3N_4 and InN growth on AlN, the changes in RHEED streak spacing occurred within the fist monolayer (ML) of growth. From the (3×3) reconstruction (determined from the spacing of fractional streaks) pattern observed on the AlN surface at the LT-InN growth temperature, we can determine that the grown AlN surface has the N polarity, i.e., the (000$\bar{1}$) surface. The InN epilayer grown on top of the N-polarity AlN has the same polarity, which is confirmed by the coherent lattice stacking sequence across the heterojunction imaged by high-resolution XTEM [Fig. 2(b)].[19] The high sample temperature (~520 °C) used for growing our InN samples is also a clear indication of N-polarity surface.[4,17]

Figure 1(c) displays the analysis from real-time video recording of RHEED patterns during the first ML growth of InN on AlN with an averaged growth rate of 24.87 s/ML. The grown lattice of AlN epilayer was confirmed by XRD and XTEM to be completely relaxed with an in-plane lattice constant of 3.11 Å, and was used as the reference in the plot of RHEED measured in-plane lattice constant of InN epilayer versus InN thickness. The RHEED analysis clearly demonstrates that the InN lattice grown on the AlN epilayer transits from pseudomorphic to commensurate growth within the first monolayer of growth, which has an important implication for the abruptness of grown heterointerface.

In Fig. 2(a), we show the XTEM image of an $InN/AlN/Si_3N_4/Si$ epitaxial structure. High crystalline quality and atomically abrupt interfaces in the structure can be clearly observed. Using the technique of selective-area electron diffraction (SAED), we confirmed the RHEED observation and found no indication of interface mixing or alloying. Figure 2(b) is a high-resolution XTEM image (color-coded) at the InN/AlN interface, showing that the interface is atomically abrupt and the lattice stacking (ABABAB…) corresponds to the wurtzite type. In addition, the atomic stacking continues without fault across the heterointerface, indicating both AlN and InN lattices have the same polarity.[19] In Fig. 3, we schematically illustrate the structural model of 8:9 commensurate match, in which every 8-unit cell of InN aligns exactly with every 9-unit cell of AlN, i.e., a common 2D commensurate superlattice is formed between InN(000$\bar{1}$) and AlN(000$\bar{1}$) planes at the interface. In comparison, the

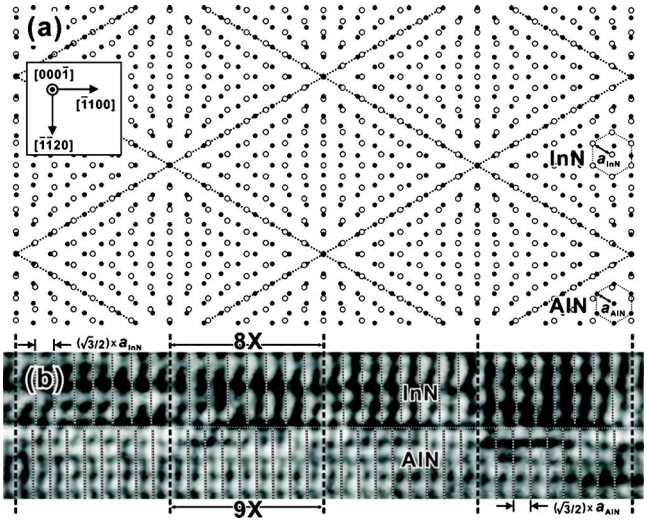

FIG. 3. (a) Schematic diagram showing the formation of a common 2D commensurate superlattice between InN(000$\bar{1}$) and AlN(000$\bar{1}$) planes. (b) A high-resolution XTEM image taken with the electron beam parallel to the $\langle\bar{1}\bar{1}20\rangle$ zone axis is shown for comparison. The 8:9 commensurate supercell is indicated by dashed lines in the schematic diagram (plan view) and the XTEM image (cross-section view).

XTEM image taken at the InN/AlN interface with the electron beam parallel to the $\langle\bar{1}\bar{1}20\rangle$ zone axis shows an excellent agreement with this commensurate model. The dislocation density determined by XTEM and atomic force microscopy in the InN films is on the order of 1×10^9 cm^{-2}. For InN grown on AlN with the commensurate match condition, the commensurate misfit strain $[\varepsilon_{com}\equiv(9\cdot a_{AlN}\text{-}8\cdot a_{InN})/8\cdot a_{InN}]$ is about -0.8% (a compressive strain). The compressive strain as well as the mismatch in thermal expansion coefficients might be the origins of the observed dislocations.

For heterostructure applications, the wurtzite-type III-nitrides provide a distinct advantage that the strong spontaneous and piezoelectric polarization effects allow the formation of 2D electron gas without intentional doping. Because that InN and AlN have a large difference in spontaneous polarization ($P_{AlN}\gg P_{InN}\approx P_{GaN}$), the heterojunction formed by InN and AlN can exhibit a stronger polarization effect than that of InN/GaN and conventional GaN/AlGaN heterojunctions. Especially, the positive interface charges induced by the difference of spontaneous polarizations (both pointing from the film to the surface normal owing to the nitrogen polarity) and the large conduction band offset at the InN/AlN(000$\bar{1}$) heterojunction can cause strong accumulation of electrons in the as-grown *n*-type InN layer to form a high-density 2D electron gas near the commensurate InN/AlN interface region. In addition, the elimination of the effects of piezoelectric field, interface roughness, and alloy scattering would allow for better control and performance of 2D electron gas. Therefore, commensurately matched InN/AlN(000$\bar{1}$) heterojunction reported here would be particularly advantageous for high-speed and possibly high-power applications of heterojunction unipolar field-effect transistors based on the superior transport properties of InN.

In summary, we have demonstrated that, despite a large difference in lattice constants, an 8:9 commensurate InN/AlN heterojunction can be formed on the technologically important Si substrate. The superior structural properties ensure that commensurately matched InN/AlN heterojunction can lead to a totally new approach toward engineering InN-based heterostructures for optoelectronic and electronic applications.

This work was supported in part by the National Science Council, Taiwan, Republic of China (NSC 94-2112-M-007-028).

[1] V. Yu. Davydov, A. A. Klochikhin, R. P. Seisyan, V. V. Emtsev, S. V. Ivanov, F. Bechstedt, J. Furthmüller, H. Harima, A. V. Mudryi, J. Aderhold, O. Semchinova, and J. Graul, Phys. Status Solidi B **229**, R1 (2002).
[2] J. Wu, W. Walukiewicz, K. M. Yu, J. W. Ager III, E. E. Haller, H. Lu, W. J. Schaff, Y. Saito, and Y. Nanishi, Appl. Phys. Lett. **80**, 3967 (2002).
[3] T. Matsuoka, H. Okamoto, M. Nakao, H. Harima, and E. Kurimoto, Appl. Phys. Lett. **81**, 1246 (2002).
[4] K. Xu and A. Yoshikawa, Appl. Phys. Lett. **83**, 251 (2003).
[5] S. Gwo, C.-L. Wu, C.-H. Shen, W.-H. Chang, T. M. Hsu, J.-S. Wang, and J.-T. Hsu, Appl. Phys. Lett. **84**, 3765 (2004).
[6] A. G. Bhuiyan, A. Hashimoto, and A. Yamamoto, J. Appl. Phys. **94**, 2779 (2003), and references therein.
[7] B. Monemar, P. P. Paskov, and A. Kasic, Superlattices Microstruct. **38**, 38 (2005).
[8] S. K. O'Leary, B. E. Foutz, M. S. Shur, U. V. Bhapkar, and L. F. Eastman, J. Appl. Phys. **83**, 826 (1998).
[9] B. E. Foutz, S. K. O'Leary, M. S. Shur, and L. F. Eastman, J. Appl. Phys. **85**, 7727 (1999).
[10] I. Vurgaftman and J. R. Meyer, J. Appl. Phys. **94**, 3675 (2003).
[11] H. Lu, W. J. Schaff, J. Hwang, H. Wu, G. Koley, and L. F. Eastman, Appl. Phys. Lett. **79**, 1489 (2001).
[12] T. Yamaguchi, Y. Saito, C. Morioka, K. Yorozu, T. Araki, A. Suzuki, and Y. Nanishi, Phys. Status Solidi B **240**, 429 (2003).
[13] A. Zur and T. C. McGill, J. Appl. Phys. **55**, 378 (1984).
[14] H. Ahn, C.-L. Wu, S. Gwo, C. M. Wei, and Y. C. Chou, Phys. Rev. Lett. **86**, 2818 (2001).
[15] C.-L. Wu, J.-L. Hsieh, H.-D. Hsueh, and S. Gwo, Phys. Rev. B **65**, 045309 (2002).
[16] C.-L. Wu, J.-C. Wang, M.-H. Chan, T. T. Chen, and S. Gwo, Appl. Phys. Lett. **83**, 4530 (2003).
[17] F. Matsuda, Y. Saito, T. Muramatsu, T. Yamaguchi, Y. Matsuo, A. Koukitu, T. Araki, and Y. Nanishi, Phys. Status Solidi C **0**, 2810 (2003).
[18] A. R. Smith, R. M. Feenstra, D. W. Greve, M.-S. Shin, M. Skowronski, J. Neugebauer, and J. E. Northrup, Appl. Phys. Lett. **72**, 2114 (1998).
[19] C. Iwamoto, X. Q. Shen, H. Okumura, H. Matsuhata, and Y. Ikuhara, J. Appl. Phys. **93**, 3264 (2003).